

# Selective removal of gold films with picosecond laser pulses

A. STRATAN, L. RUSEN\*, M. ULMEANU, C. FENIC, R. DABU

Department of Lasers, National Institute for Laser, Plasma, and Radiation Physics, 409 Atomistilor St., PO Box MG-36, 077125 Bucharest, Romania

Picosecond laser ablation of thin gold films has been investigated by using the second-harmonic output of a Nd:YAG laser. An *in situ* calibration-method for laser pulses with Gaussian spatial profile is described and then applied to determine the pulse peak-fluence incident on the films surface. For 200-nm gold films (150-nm Au + 50-nm Cr on silicon substrate) irradiated with 400-ps Gaussian laser pulses at 532-nm wavelength, a peak-fluence of 0.53 J/cm<sup>2</sup> at the ablation threshold was measured, and a selective, single-shot removal of the gold layer was obtained in the 2-4 J/cm<sup>2</sup> peak-fluence range.

(Received September 11, 2009; accepted January 19, 2010)

**Keywords:** Picosecond laser, Fluence calibration, Gold film, Selective removal

## 1. Introduction

Picosecond laser pulses can machine many industrial relevant materials with minimal thermal influences. No micro-cracks, minimal debris or recast layer, and no damage to adjacent structures are observed. Picosecond lasers are usually much less complex, compared to femtosecond lasers, more reliable, and their usage is less expensive. Finally, their outputs can be efficiently converted to shorter wavelengths in nonlinear crystals to get energetic ultrashort pulses in the green and in the ultraviolet. With these advantages, picosecond lasers can be the best choice today for many micromachining applications, particularly in the low fluence regime. A majority of micro-machining applications uses a low ablation-fluence for the processing of surfaces, films and thin sheets [1, 2, 3]. In these applications, the highest quality is achieved with pulse energy just above ablation threshold (e.g. in the J/cm<sup>2</sup> range for metal machining). The ablation depth of only a few hundred nm for every pulse provides *fine* controlled material removal.

Absolute calibration of the delivered laser fluence is essential for quantitative studies of laser interaction with materials. The accuracy of this calibration depends primarily on the measurement of the focused-beam spot size on the sample surface. The scanning knife-edge technique for the measurement of Gaussian beam radii has been used earlier to measure micron sized Gaussian beams [4]. J. M. Liu has used a more simple fitting-procedure for measurements of focused Gaussian-beam spot-sizes, by using pulse-fluence dependence of the measured damage radii on silicon-crystal surface [5].

This contribution will be split into two parts. In the first part we report a method for absolute calibration of the peak-fluence for focused laser pulses with Gaussian spatial profile, based on pulse-energy dependence of the crater diameter ablated on the sample surface. We derive a simple relation between the diameter of an ablated crater

and the material dependant ablation threshold fluence, the laser  $1/e^2$  beam diameter, and the peak fluence in the Gaussian laser beam. By fitting the measured crater diameters versus pulse-energy to the theoretical dependence, both the ablation threshold and  $1/e^2$  laser spot size are simultaneously determined. This method will be applied in the second part to study the ablation of 200-nm gold films irradiated with 400-ps Gaussian pulses at 532-nm wavelength.

## 2. Calibration method

As is well known, for a Gaussian beam, the transversal fluence profile  $F(r)$  is given by

$$F(r) = F_0 \exp(-8r^2 / d_0^2) \quad (1)$$

where  $r$  represents the distance from the beam center,  $d_0$  is the  $1/e^2$ -diameter of the Gaussian fluence profile and  $F_0$  denotes the peak laser fluence at the cross-sectional surface. The peak fluence and the total pulse energy  $E$  are directly related by

$$F_0 = \frac{8E}{\pi d_0^2} \quad (2)$$

because  $E$  is the integrated value of the Gaussian profile of laser fluence over the irradiated area with a radius  $d_0/2$ . When the peak fluence of a Gaussian laser spot applied to the sample surface exceeds the material-dependant ablation threshold fluence  $F_{th}$ , a crater is ablated in the central region of the laser spot. The diameter

$d$  of the ablated crater can be determined from the condition

$$F(r = d/2) = F_{th} \quad (3)$$

Using (1) and (3), the diameter of an ablated crater can be related to the laser parameters  $F_0$  and  $d_0$ , and to the material-dependant parameter  $F_{th}$

$$d^2 = \frac{d_0^2}{2} \ln(F_0 / F_{th}) \quad (4)$$

Because of the linear dependence of the peak fluence on the pulse energy, the equation (4) is equivalent to

$$d^2 = \frac{d_0^2}{2} \ln(E / E_{th}), \quad (5)$$

where  $E_{th}$  is the threshold pulse energy corresponding to  $F_{th}$  (2). Because of the linear dependence of the square of the crater diameters  $d^2$  on the natural logarithm of the laser pulse energy  $E$ , it is possible to determine both the laser parameter  $d_0$  and the material parameter  $E_{th}$  from a semilog plot of  $d^2$  versus  $E$ . The beam-diameter parameter is given by the slope of the fitted straight line of this plot, and the threshold pulse energy can be calibrated from the intercept of this line on the horizontal axis. Now, using (2), it is possible to accurately calibrate the threshold fluence  $F_{th}$  and the peak-fluence  $F_0$ .

The method described above is very useful for calibration of the laser fluence on highly focused beam spots, eliminating the need to directly measure such small-size spots, which is a difficult and unreliable task. An accurate determination of the focused beam size is vital for laser microprocessing, because the peak-fluence of a Gaussian pulse is the most meaningful energetic quantity, rather than just the pulse energy.

### 3. Results and discussion

In this part, mainly the results obtained at study of gold films ablation will be described. The measured ablation threshold fluence of the gold films is compared to theoretical evaluation and to reported experimental data.

The gold films used in our experiments are 150 nm thick, coated on a silicon substrate over an intermediate chromium layer with a thickness of about 50 nm. Chromium was used to ensure the adhesion of Au films on silicon. To ablate the film samples, we use a home-made picosecond Nd:YAG laser that delivers linearly polarized pulses of 400-ps duration at 532-nm wavelength and maximum 10-Hz rate, in a nearly TEM<sub>00</sub> Gaussian mode

[6]. The radial spatial intensity profile of the green beam is shown in Fig. 1.

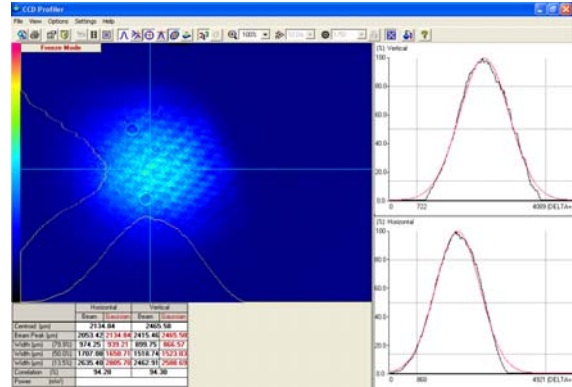
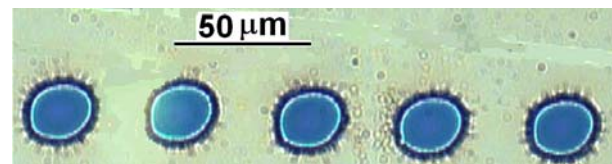


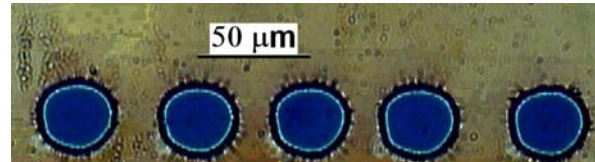
Fig. 1. Spatial intensity profile of the 532-nm laser output at 7-mJ pulse energy, 2-Hz pulse rate.

The samples surface was placed vertically, in the focal plane of a focusing lens ( $f = 75$  mm). The beam was directed perpendicularly on the processed surface, and the ablation was performed under atmospheric pressure. The energy of each laser pulse was measured with a pyroelectric detector, by using a calibrated reflection from a beam-splitter. The energy stability of the green laser pulses was typically 2% rms.

A three-axis micrometer translation stage allowed precise positioning of the processed sample. A high-resolution surface profilometer (0.5-nm step height repeatability) is used to measure the depth and the diameter of the ablated craters. The mean value of the squared diameter is obtained by averaging over five craters processed at a constant pulse-energy in single-shot regime, as shown in Fig. 2.



(a)



(b)

Fig. 2. Microscope photograph of single-shot ablation craters processed in Au films. The spacing between two craters (from center to center) is 50- $\mu$ m. (a) Laser pulse-energy  $E = 10 \mu$ J, average crater diameter  $d = 25.6\text{-}\mu$ m. (b)  $E = 20 \mu$ J,  $d = 30\text{-}\mu$ m.

Fig. 3 shows the mean value  $d^2$  versus the natural logarithm of the laser pulse energy  $E$ . The slope of the linear fit to the data points yields a beam diameter  $d_0$  around 25  $\mu\text{m}$ , and the extrapolation of  $d^2$  to zero value yields an ablation threshold energy  $E_{th}$  of 1.2  $\mu\text{J}$ , corresponding to an ablation threshold fluence  $F_{th}$  of 0.53  $\text{J}/\text{cm}^2$ . For this fitting procedure, our estimated absolute uncertainty in fluence was 10%. Taking into consideration that the threshold fluence is proportional to the laser wavelength [7], this value is in agreement with the reported damage thresholds measured at 1053-nm laser wavelength and 400-ps pulse-duration on 200-nm gold films deposited onto photoresist [8].

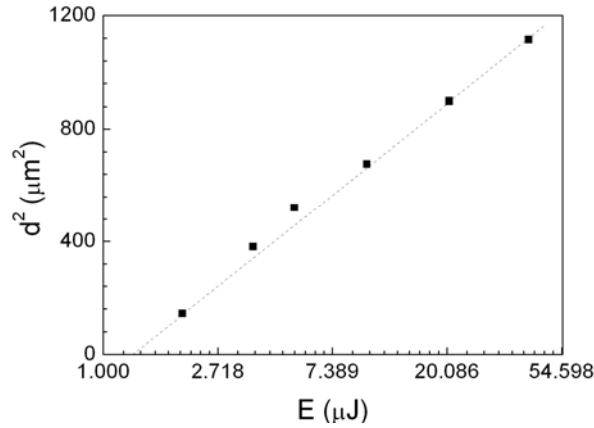


Fig. 3. Squared diameter  $d^2$  of the ablated craters in Au films as a function of the laser pulse energy  $E$  (400 ps pulse-duration,  $\lambda = 532$  nm). The dashed line represents the least-squares-fit according to (5).

For laser pulse durations  $t_p > 10$  ps, the heat conduction and hydrodynamic motion dominate the ablation process. Initially, the laser energy is absorbed by the electrons. The electrons thermalize in about 100 fs. Thermal equilibrium between the electrons and the lattice (the ions) occurs after a multiple of the electron-phonon relaxation time. Typical electron-phonon relaxation times are 0.5 – 50 ps. For metals, the time that is necessary for the electron energy transfer to the ions is estimated at 20–30 ps [9]. For pulse durations of hundred picosecond or longer, the electrons and the lattice (the ions) are in equilibrium early in the beginning of the laser pulse. The ablation threshold for this case is defined by condition that the absorbed laser energy is fully converted into the energy of broken atomic bonds in a layer with the thickness of the heat diffusion depth  $l_{heat} \sim (\kappa\kappa_p)^{1/2}$  during the laser pulse [7]:

$$F_{th} \approx \frac{(\kappa\kappa_p)^{1/2} \varepsilon_b n_a}{A}, \quad (6)$$

where  $A$  is the Fresnel absorption coefficient near the ablation threshold of the material,  $\kappa$  is the thermal diffusivity,  $\varepsilon_b$  the heat of evaporation per atom (e.g. atomic binding energy),  $n_a$  the number density of the atoms.

In the ablation condition, it is difficult to estimate the Fresnel absorption coefficient of the target, because the real and imaginary parts of the dielectric permittivity, and thus, the electron-plasma frequency and the effective collision frequency of electrons with ions, all are laser-intensity and time dependent. For metals, near the ablation threshold, the absorption coefficient  $A$  can be approximated as the following [7]:

$$A \approx \left( \frac{8\omega}{\omega_{pe}} \right)^{1/2} \left\{ 1 - \left( \frac{\omega}{2\omega_{pe}} \right)^{1/2} \right\}, \quad (7)$$

where the electron plasma frequency  $\omega_{pe}$  is a material parameter, and  $\omega$  is the frequency of the incident laser pulse.

Thermal diffusivities of gold films deposited on a chromium intermediate layer were measured using the technique of transient thermal gratings [10]. In the film thickness range from 100 nm to 2  $\mu\text{m}$  an average value of  $\kappa(\text{Au}) = 0.39 \text{ cm}^2\text{s}^{-1}$  was found, and no trends with film thickness was observed. This number amounts to only about 1/3 of the Au bulk value and is much closer to one for Cr bulk ( $0.30 \text{ cm}^2\text{s}^{-1}$ ), supporting the suspicion that the Cr intermediate layer badly distorts the thermal diffusion data of the Au films. The Au-Cr double layer seems to behave optically like gold and thermally like chromium [10].

For an Au-Cr film ( $\varepsilon_b = 3.37$  eV/atom,  $n_a = 5.9 \times 10^{22} \text{ cm}^{-3}$ ,  $\omega_{pe} = 1.876 \times 10^{16} \text{ s}^{-1}$  [7],  $\kappa = 0.39 \text{ cm}^2\text{s}^{-1}$  [10]) evaporated by a laser pulse of 532-nm wavelength ( $\omega = 3.58 \times 10^{15} \text{ s}^{-1}$ ,  $t_p = 400$  ps), the Fresnel absorption coefficient from Eq. (7) is  $A = 0.85$ , the ablation threshold from Eq. (6) is  $F_{th} \approx 0.47 \text{ J}/\text{cm}^2$ , with an heat diffusion depth  $(\kappa\kappa_p)^{1/2} = 125 \text{ nm}$ .

A reproducible and selective removal of the gold layer was obtained in the peak-fluence range of 2–4  $\text{J}/\text{cm}^2$ , as shown in fig. 4a, 4b, 4c. For selective removing of the gold layer, a single-shot ablation rate of maximum 1.5 ng per pulse was measured at 4  $\text{J}/\text{cm}^2$  peak-fluence.

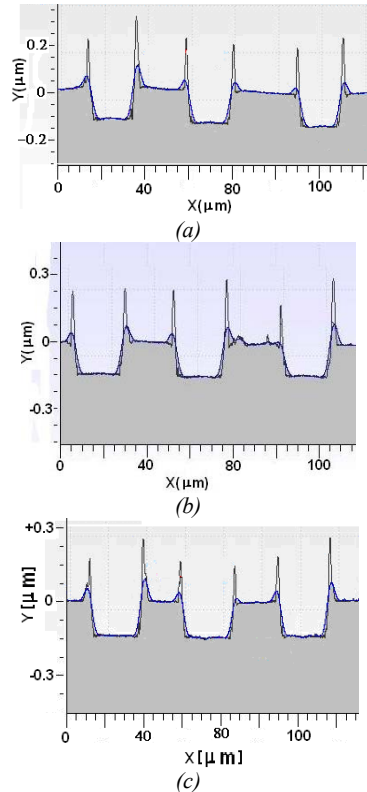


Fig. 4. Profilometer cross-sections of single-shot ablated craters in 150-nm Au layers (400-ps laser pulse-duration at 532-nm wavelength). (a) crater depth  $\delta \approx 140$ -nm, laser peak-fluence  $F_0 = 1.5 \text{ J/cm}^2$ ; (b)  $\delta = 150$ -nm,  $F_0 = 2 \text{ J/cm}^2$ ; (c)  $\delta = 150$ -nm,  $F_0 = 4 \text{ J/cm}^2$ ;

To remove also the Cr layer, it was necessary to apply a second pulse (Fig. 5). The cross-sections profiles of the ablated craters shown in Figs. 4 and 5 were measured just after the laser irradiation, without ultrasonic cleaning of the processed samples.

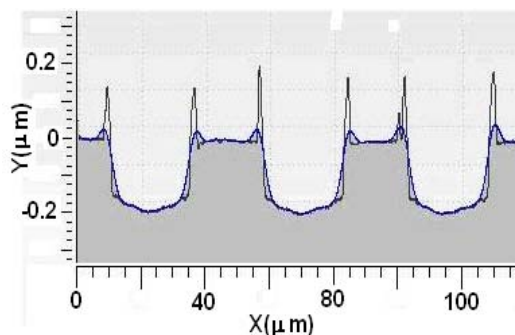


Fig. 5. Profilometer cross-sections of two-shots ablated craters through both Au and Cr layers;  $\delta \approx 200$ -nm,  $F_0 = 4 \text{ J/cm}^2$ .

#### 4. Conclusions

We have demonstrated the selective removal of thin gold films by single-shot ablation with short visible laser pulses of 400-ps duration and 532-nm wavelength. The laser fluence applied on the films surface has been calibrated in-situ, by using the linear semilog relationship between the square of the ablated crater-diameter and the energy of a laser pulse with Gaussian spatial beam profile.

For 200-nm gold films ( 150-nm gold layer coated on silicon substrate over an intermediate Cr-layer of 50-nm thick ), a laser peak-fluence of  $0.53 \text{ J/cm}^2$  was measured at the ablation threshold. This value was found in agreement with theoretical estimations and reported experimental data. A selective, single-shot removal of the gold layer was obtained in a relatively large laser fluence range of  $2\text{-}4 \text{ J/cm}^2$ .

#### References

- [1] B. Gu, in Proc. of SPIE 5714-04, 2005.
- [2] Liu, X., in Proceedings of SPIE 5713-56, 2005.
- [3] A. Nebel et al., Photonics West, LASE Conference: Commercial and Biomedical Applications of Ultrafast Lasers VI Paper No. 6108-37, 2006.
- [4] Y. Suzuki, A. Tachibana, Appl. Opt. **14**(12), 2809 (1975).
- [5] J. M. Liu, Opt. Lett. **7**(5), 196 (1982).
- [6] A. Stratan, L. Rusen, R. Dabu, C. Fenic, C. Blanaru, J. Optoelectron. Adv. Mater. **10**(11), 3022 (2008).
- [7] E. G. Gamaly, A. V. Rode, V. T. Tikhonchuk and B. Luther-Davies, CLEO-Europe'2000, papers QMD6 and CTuK114 (2000); [http://laserspark.anu.edu.au/Pubs/gamaly\\_02\\_ablation.pdf](http://laserspark.anu.edu.au/Pubs/gamaly_02_ablation.pdf)
- [8] Stuart et al., J. Opt. Soc. Am. B Vol. **13**(2), 459 (1996).
- [9] S. Nolte, J. Opt. Soc. Am. B/ Vol. **14**(10), 2716 (1997).
- [10] E. Matthias, Appl. Phys. A **58**, 129 (1994).

\*Corresponding author: laurentiu.rusen@infpr.ro